Journal of Molecular Structure 1215 (2020) 128291

Contents lists available at ScienceDirect

Journal of Molecular Structure

journal homepage: http://www.elsevier.com/locate/molstruc

Spectroscopic characterization and efflux pump modulation of a thiophene curcumin derivative

Mauro M. Oliveira [a, *], Helcio S. Santos [a, b], Henrique D.M. Coutinho [a], Paulo N. Bandeira [b], Priscila T. da Silva [a], Thiago S. Freitas [a], Janaina E. Rocha [a], Jaize C. Xavier [a], Fabia F. Campina [a], Cristina R.S. Barbosa [a], José B. Araújo Neto [a], Raimundo L.S. Pereira [a], Maria M.C. Silva [a], Débora F. Muniz [a], Alexandre M.R. Teixeira [a, c], Vanessa M. Frota [b], Tigressa H.S. Rodrigues [b], Ana M. Amado [d], Maria P.M. Marques [d, e], Luis A.E. Batista de Carvalho [d], Carlos E.S. Nogueira [a, c, d]

[a] Department of Biological Chemistry, Regional University of Cariri, Crato, CE, Brazil
[b] Science and Technology Centre - Course of Chemistry, State University Vale Do Acaraú, Sobral, CE, Brazil
[c] Department of Physics, Regional University of Cariri, Crato, CE, Brazil
[d] Universidade de Coimbra, Unidade de I&D Quimica-Física Molecular (QFM-UC), Department of Chemistry, 3004-535 Coimbra, Portugal
[e] Universidade de Coimbra, Department of Life Sciences, 3000-456, Coimbra, Portugal

ARTICLE INFO

Article history:
Received 15 March 2020
Received in revised form
16 April 2020
Accepted 16 April 2020
Available online 21 April 2020

Keywords:
Curcumin
Chalcone
Efflux pump
DFT
Spectroscopy
Docking

ABSTRACT

Curcumin, along with its derivatives, form a large class of natural and synthetic compounds with notable biological activity. However, their highly reactive β-diketone moiety renders this type of compounds unstable at pH above 6.5. The substitution of this group for a mono-carbonyl solves this problem, while improving antibacterial and anti-inflammatory activities. A thiophene curcuminoid, (1E,4E)-1,5-Di(thiophen-2-yl)penta-1,4-dien-3-one (DB Thiophene), has been synthesised and its molecular and spectroscopic characterization is reported, as well as a complete vibrational assignment. An efflux pump inhibition assay determined that DB Thiophene exhibits a remarkable NorA and MepA efflux pump inhibition activity. Molecular docking studies were carried out in order to understand this inhibition mechanism.

1. Introduction

Curcumin is a polyphenol (Scheme 1) and an active principle of the *Curcuma longa* herb, also known as turmeric. Its derivatives, called curcuminoids, form a large class of natural and synthetic compounds with notable biological activity [1]. Curcumin interacts with numerous targets, such as transcription and growth factors and their receptors, as well as genes that regulate cell proliferation and apoptosis [2]. It has thus been widely used as a chemo-preventive agent [2] and it is a prime candidate for cancer treatment. In fact, it can suppress the tumorigenic activity of a variety of carcinogens in the colon, duodenum, oesophagus, stomach, breast, and prostate. Curcumin and its derivatives are also known to suppress the growth of bacteria of several genera, such as Streptococcus, Staphylococcus, Lactobacillus and Helicobacter [3]. Additionally, it exhibits antiviral activity, including anti-HIV through inhibition of the HIV-1 integrase, an enzyme needed for viral replication [4].

The potential of curcumin is only hampered by its poor bioavailability and pharmacokinetic profile, as its highly reactive diketone moiety makes it unstable *in vitro* at pH above 6.5 [5]. Several studies have focused on finding synthetic derivatives with improved pharmacokinetic profiles [6,7] by substitution of the β-diketone moiety for a mono-carbonyl one. It has been shown that this substitution not only improves stability, but also leads to a better antibacterial and anti-inflammatory activities [8,9]. Likewise,

* Corresponding author. Department of Biological Chemistry, Regional University of Cariri, Campus Pimenta II, CEP: 63, 100-000, Crato, CE, Brazil.
E-mail addresses: mauropandi@gmail.com, mauro.oliveira@fapce.edu.br (M.M. Oliveira).

https://doi.org/10.1016/j.molstruc.2020.128291
0022-2860/

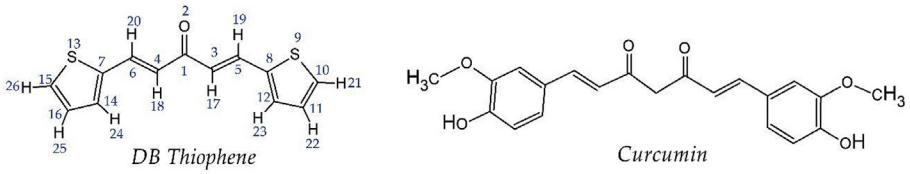

Scheme 1. DB Thiophene structure and atom numbering along with Curcumin structure.

modifications of the aromatic rings substitution also seems to improve the biological activity of curcumin derivatives [10].

The use of new substances in the fight against bacterial infections is often accompanied by increased resistance of these organisms. There are several mechanisms of resistance to antibiotics, one of them being known as efflux pump. This active efflux is able to extrude different compounds from the cell and is therefore seen as a key element in antimicrobial resistance. Currently, more than ten multidrug efflux pump types have been identified for *S. aureus* [11], namely NorA and MepA.

NorA is a fluoroquinolone-resistant efflux pump that expels a set of different antibiotics and other substances, such as norfloxacin, ciprofloxacin, ethidium bromide and quaternary ammonium compounds [12–14]. MepA belongs to the multidrug and toxin extrusion (MATE) efflux pump family. First described by Kaatz et al. [15], it is also found in *S. aureus* mutant strains. Inhibition of the efflux pumps can be achieved by reducing the pump gene expression, interrupting pump assembly, reducing substrate binding by competitive or non-competitive means and disrupting the pump's required energy source. Compounds that are capable of performing such inhibition are called efflux pump inhibitors (EPI) [16].

Since chalcone derivatives with a heterocyclic thiophene ring have an increased antibacterial activity [17], a mono-carbonyl curcumin derivative with thiophene instead the usual aromatic rings was synthesised - the (1E,4E)-1,5-Di(thiophen-2-yl)penta-1,4-dien-3-one, henceforth denominated DB thiophene (Scheme 1). This curcuminoid was fully characterised by NMR, Raman and IR spectroscopies, with a complete assignment of bands based on frequency calculations using the DFT approach. In order to test the ability of DB thiophene as an EPI, inhibition tests focused on *S. aureus* strains were performed. The inhibition mechanism of the NorA efflux pump was then studied by means of molecular docking using a NorA protein homolog model.

2. Materials and methods

2.1. Materials

Potassium hydroxide was purchased from Dinâmica Química Contemporânea Ltd. (Indaiatuba, Brazil). Ethanol and acetone were obtained from Vetec Química Fina Ltd (Duque de Caxias, Brazil). Chlorpromazine (CPZ), ciprofloxacin, norfloxacin, carbonyl cyanide m-chlorophenylhydrazone (CCCP), thiophene-2-carbaldehyde and ethidium bromide (EtBr) were acquired from Sigma Aldrich Brasil Ltd. (São Paulo, Brazil). Brain heart infusion (BHI) was purchased from KASVI company (São José do Pinhais, Brazil).

2.2. Synthesis

The (1E,4E)-1,5-Di(thiophen-2-yl)penta-1,4-dien-3-one was synthesised by the Claisen–Schmidt condensation method [18,19], with thiophene-2-carbaldehyde instead of benzaldehyde. In an Erlenmeyer flask containing 50 mL of KOH 10% (*m/v*) and 40 mL of ethanol, 7 mL of thiophene-2-carbaldehyde:acetone (5:2) was slowly added, under agitation, and the temperature was kept at 0 °C. After 30 min, the mixture was filtered: a precipitate was obtained and washed with small portions of distilled water. The compound was redissolved in hot ethanol, filtered and allowed to cool in an ice bath. The formed crystals were washed with cold ethanol and dried at room temperature. Scheme 2 shows the DB Thiophene synthesis reaction.

(1H NMR (CDCl3, 500 MHz): δ = 7.48 (2H, d, J = 5.1 Hz, H21, H25), 7.15 (2H, m, H22, H26), 7.40 (2H,d, J = 3.6 Hz, H23,H24), 6.89 (2H, d, J = 15.6 Hz, H17, H18), 7.92 (2H, d, J = 15.6 Hz, H19, H20) 13C NMR (CDCl3, 125 MHz): δ = 140.3 (CH, C7, C8), 128.4 (CH, C10, C15), 128.8 (C11, C16), 135.6 (CH, C12C14), 124.4 (CH, C3, C4), 131.8 (CH, C5, C6), 187.7 (C, C1)); EIMS *m/z* (M+. 246), calcd for: C13H10OS2/246.

2.3. Vibrational spectroscopy

The Raman spectrum was recorded using compacted powder in the sample holder of a Bruker RAM II FT-Raman module, equipped with a liquid nitrogen cooled high-sensitivity Ge detector, and coupled to a Bruker Optics VERTEX 70v FTIR spectrometer. The 1064 nm line of a Nd:YAG laser was used as the excitation radiation, with a nominal laser power of 150 mW. The spectrum was the sum of 60 scans, at a typical resolution of ca. 4 cm^{-1}.

The FTIR-ATR spectrum was measured at room temperature using a spectrometer Bruker Vertex 70v equipped with a RT-DLaTGS (Deuterated Lanthanum α-Alanine doped TriGlycine Sulphate) detector and a Wide Range MIR-FIR. The spectra were recorded in the region 130 to 4000 cm^{-1} with a resolution of 2 cm^{-1} and accumulating 32 scans *per* spectrum. A Blackman–Harris three-term apodization function and the Mertz search phase correction algorithm were used.

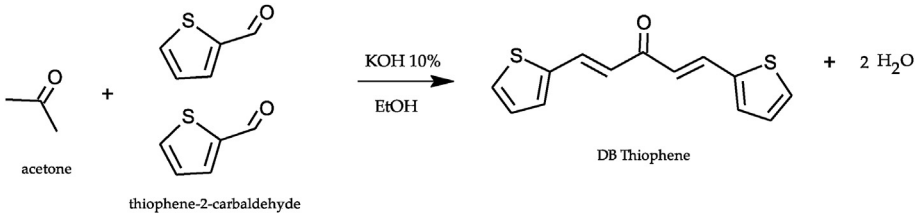

Scheme 2. DB Thiophene synthesis reaction.

2.4. NMR and GC-MS

The chemical reagents were from Sigma-Aldrich. 1H and 13C NMR spectra were obtained using a Bruker Spectrometer, model Avance DPX - 300 and model Avance DRX-500 operating at a frequency of 300 MHz and 500 MHz for hydrogen, 75 MHz and 125 MHz for carbon respectively. The spectra were measured in $CDCl_3$ solvents at 27 °C and chemical shifts are reported as δ values in parts per million (ppm) relative to tetramethylsilane (δ 0.00) as the internal standard. The mass spectra were obtained with a Shimadzu QP201 GC-MS (Gas Chromatography coupled to Mass Spectrometry) using RTX-5MS capillary column (30.0 m × 0.25 mm x 0.30 mm) for compounds within the literature record.

2.5. Computational details

Density Functional Theory (DFT) calculations [20] were performed using the Gaussian 09 program [21]. Initial coordinates were generated according to the NMR results. The B3LYP exchange-correlation functional [22] was applied, combined with the 6-31G* basis set. All geometries were fully optimised within the Berny algorithm, using redundant internal coordinates and considering the Gaussian default convergence criteria. Vibrational wavenumber calculations were carried out for the optimised geometries, at the same theory level, to verify convergence to a real minimum within the potential energy surface (no negative eigenvalues) and to assist in the vibrational mode description.

For an accurate comparison between the calculated and experimental vibrational wavenumbers, the former were corrected for anharmonicity and incomplete electron correlation treatment, using the scaling factors of 0.960 [23] and 0.942 for predicted values below and above 2000 cm^{-1}, respectively. Vibrational modes were analysed, in terms of their Potential Energy Distribution (PED), using the VEDA [24] program with default optimisation options.

2.6. Evaluation of efflux pump inhibition by MIC reduction

The evaluation of the efflux pump inhibition was performed according to Tintino et al. [12]. The two strains of *S. aureus* used were: SA-1199 B, which overexpresses the NorA gene encoding the NorA efflux protein and the multi-drug resistant (MDR) mutant strain SA-K2068 which presents the MepA efflux pump. The strains were maintained on blood agar base slants and, prior to use, the cells were grown overnight at 37 °C in Heart Infusion Agar slants.

Chlorpromazine (CPZ), carbonyl cyanide m-chlorophenylhydrazone (CCCP) and ethidium bromide (EtBr) were used for this essay. Norfloxacin and Ciprofloxacin were the antibiotics used for NorA and MepA efflux inhibition respectively. The antibiotics and DB Thiophene were dissolved in dimethyl sulfoxide aqueous solution (5.1%, v/v). The CPZ and EtBr were dissolved in sterile water and CCCP in methanol/water (1:1, *v/v*). All the compounds were stored at −20 °C, at a final concentration of 4162.60 μM for DB Thiophene, 5004.50 μM for CCCP, 3211.44 μM for CPZ, 2597.00 μM for EtBr, 3206.71 μM for norfloxacin and 3090.48 μM for ciprofloxacin.

The Minimal Inhibitory Concentration (MIC) is defined as the lowest concentration in which no growth can be observed [25]. The MIC's of CPZ, CCCP, EtBr and DB Thiophene were obtained in a microdilution assay using 150 μL of each strain suspended in saline solution, corresponding to a final concentration of 10^5 colony-forming units/mL, followed by addition of 1350 μL of brain heart infusion (BHI) broth. Aliquots of 100 μL were transferred to a 96-well multiplate with two-fold serial dilutions by adding 100 μL of each compound solutions with final concentrations ranging from 2.03 to 2081.00 μM for DB Thiophene, 2.44–2502.25 μM for CCCP, 1.57–1605.72 μM for CPZ and 1.27–1298.50 μM for EtBr. The trays were incubated at 37 °C for 24 h and bacterial growth was revealed by staining with resazurin.

In order to evaluate the potential inhibition of the efflux pump by DB Thiophene, a comparative study was made assessing its ability to decrease the MIC antibiotics and EtBr (substrate for MDR pumps including NorA [11,13,26,27] and MepA [15,28]), by comparing with CPZ and CCCP which are standard EPI's [29–32]. Eppendorf's were prepared with the EPI's and DB Thiophene at a sub-inhibitory concentration (MIC/8), which corresponds to 520.32 μM for DB Thiophene, 625.56 μM for CCCP and 401.43 μM for CPZ. Then 100 μL of the Eppendorf's content were transferred to a 96-well microtiter tray with two-fold serial dilution by adding 100 μL of antibiotics and EtBr with a final concentration ranging from 1.27 to 1298.50 μM for EtBr, 1.56–1603.36 μM for norfloxacin and 1.50–1545.24 μM for ciprofloxacin. The trays were incubated for 24 h at 37 °C and bacterial growth was revealed by staining with resazurin.

2.7. Statistical analysis of the microbiological results

Antibacterial assays were performed in triplicate and results were expressed as an average of the replicates. The results of the tests are expressed as the geometric mean. Statistical hypothesis analysis was applied using a Two-Way ANOVA followed by the Bonferroni post hoc test (using the GraphPad Prism 5.0 [33] software).

2.8. Docking

The NorA sequence of *S. aureus* 1199 strain (Entry Q03325) was retrieved from the Universal Protein Resource database (Uniprot). The web-based SWISS-MODEL [34] service was used to build a homology model of NorA. The HHblits-based automated mode was used, resulting in 50 different templates, the best one being based on the structure of the *E. coli* YajR transporter (PDB-ID: 3wdo).

The grid box for the docking procedure was defined as an 80Åx80Åx80 Å box around the geometrical center of the NorA model. Partial Gasteiger charges were added to ligand atoms while non-polar hydrogen atoms were mixed and rotational bonds determined. Docking studies were carried out using the Lamarckian genetic algorithm in Autodock 4.0 [35]. All other parameters were kept at their default values. The ten best results were chosen by least binding energy.

3. Results and discussion

3.1. Structural and conformational analysis

Fig. 1a and b and displays the ^1H NMR and ^{13}C NMR spectra of DB Thiophene, respectively. The NMR profile (Fig. 1a) shows two doublets, one at 6.89 ppm, assigned to H17 and H18 (J = 15.6 Hz), and another at 7.92 ppm, due to H19 and H20 (J = 15.6 Hz). Their coupling constants confirm the stereochemistry E of the double bond. The signals at 7.48 (d, J = 5.1 Hz), 7.40 (d, J = 3.6 Hz) and 7.15 ppm (m) are ascribed to the hydrogens of the thiophene ring. In the ^{13}C spectra the signal from the unsaturated carbonyl is at 187.7 ppm, while the ketone peak is seen at 203.8 ppm. However, the presence of unsaturation causes a shift of the latter to high field. The charge delocalisation is either caused by the aromatic ring (thiophene) or by the double bond, rendering the carbonylic carbon less electron deficient. The olefinic carbons C3 and C4 are observed at 124.4 ppm, while C5 and C6 appear at 131.8 ppm. The carbon atoms belonging to the thiophene rings are at 140.3, 135.6, 128.8 and 128.4 ppm. The chromatogram (Fig. S1) confirms the presence

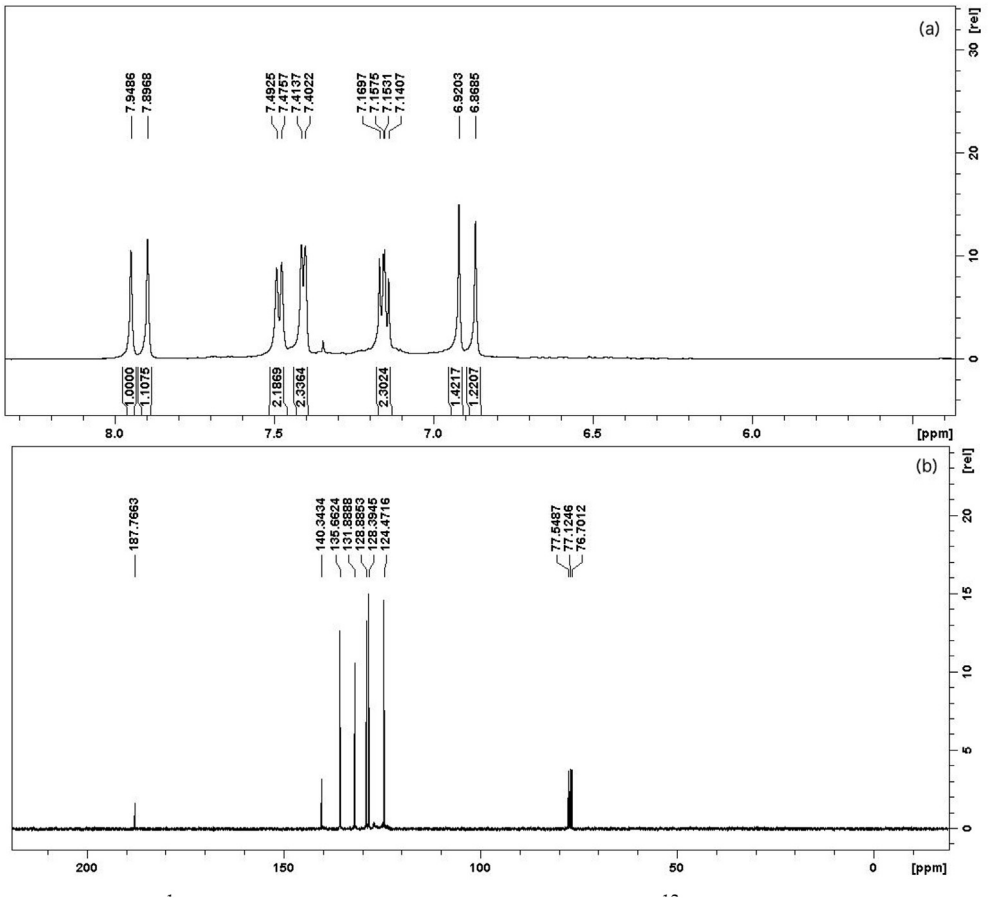

Fig. 1. (a) ^{1} H NMR Spectrum of DB thiophene (b) ^{13} C NMR Spectrum of DB Thiophene.

of only one compound, thereby indicating the analytical purity of chalcone. ESIMS and a proposed fragmentation scheme are provided as supplementary material as Fig. S2 and Scheme S1, respectively.

Rotations around the single bonds of the enone groups lead to three possible conformational isomers, namely: *cis-cis*, *cis-trans* and *trans-trans* isomers, henceforth denominated C0, C1 and C2, respectively (Fig. 2). DFT calculations performed on the isolated molecule show that the *trans-trans* conformation, *i.e.* the C2 conformer, is the preferred geometry (at least *in vacuum*). The calculated SCF (self-consistent field method) energies for the C0 and C1 isomers are 10.0 and 5.0 kJ/mol higher, respectively. This is consistent with the crystal structure reported by Murugavel et al. [36], in which the asymmetric unit of the compound was found to be in *trans-trans* conformation.

3.2. Vibrational analysis

The DB thiophene molecule contains 26 atoms, yielding 72 vibrational modes. The Raman and IR spectra of the compound, as well as the calculated spectra for the considered conformers are shown in Fig. 3a and b. Comparison of spectra for wavenumbers higher than 2000 cm^{-1} are given in Figs. S3 and S4 (Supplementary information).

The calculated Raman profile of C1 is the one which matches more closely the experimental data, although the three conformers of the compound exhibit almost the same modes at roughly the same frequencies, within 10 cm^{-1} of each other, which hardly affects the overall assignment. These differences will be discussed

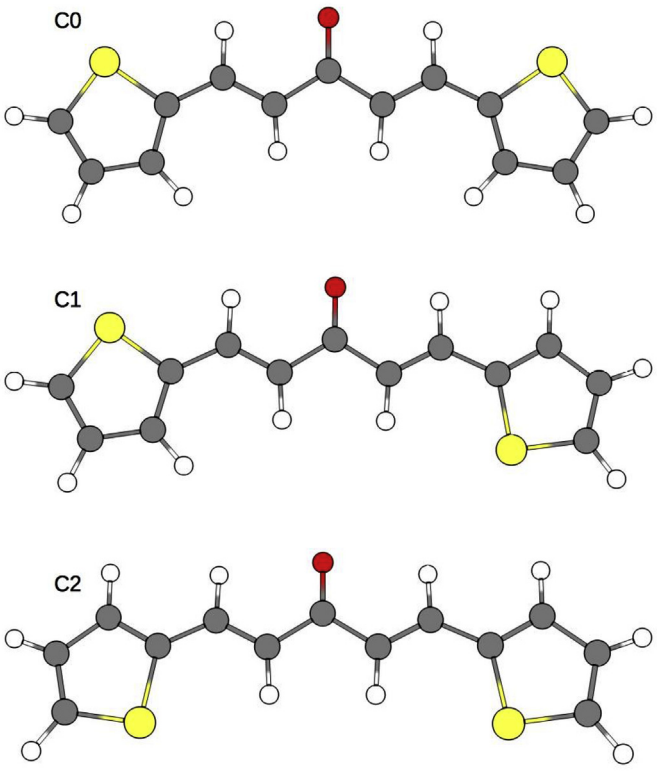

Fig. 2. Representation of the three conformers of DB thiophene.

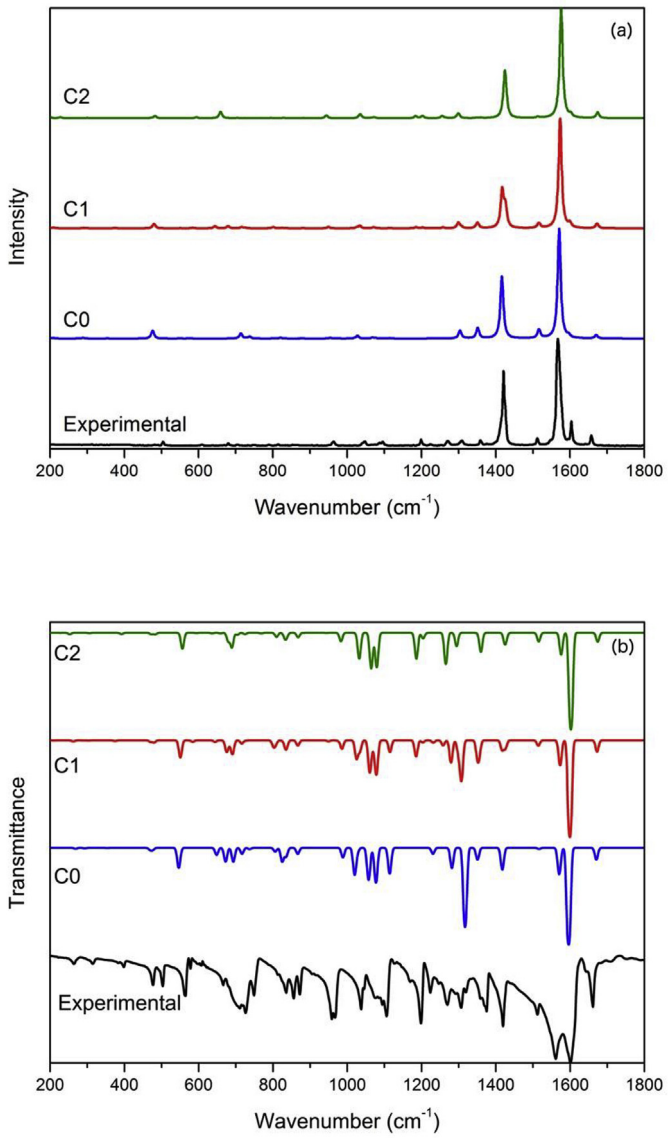

Fig. 3. Raman (a) and IR (b) spectra of DB thiophene.

Table 1
Observed (Raman and Infrared) and calculated vibrational wavenumbers (cm^{-1}) for Thiophene (C1).

ω_{IR}	ω_{Raman}	ω_{Calc}	Assignment
3088	3088	3081	$\nu(CH)_{ring}$
3071	3074	3079	$\nu(CH)_{ring}$
3044		3047	$\nu(CH)_{ring}$
3013	3012	3034	$\nu(CH)_{ring}$
	2990	2900	$\nu(CH)_{enone}$
1662	1658	1673	$\nu(OC)_{enone} + \nu(CC)_{enone}$
1602	1604	1599	$\nu(CC)_{enone}$
1562	1567	1573	$\nu(OC)_{enone} + \nu(CC)_{enone}$
1512	1512	1517	$\nu(CC)_{ring} + \delta(HCC)_{ring}$
	1425	1426	$\nu(CC)_{ring} + \delta(HCC)_{ring}$
1419	1420	1417	$\nu(CC)_{ring} + \delta(HCC)_{ring}$
1376	1376	1355	$\nu(CC)_{ring} + \delta(HCS)_{ring} + \delta(HCC)_{ring}$
1359	1359	1351	$\nu(CC)_{ring} + \delta(HCS)_{ring}$
1319		1307	$\nu(CC)_{enone} + \delta(HCC)_{enone}$
1307	1309	1299	$\nu(CC)_{enone} + \delta(HCC)_{enone}$
1270	1271	1258	$\delta(HCC)_{enone} + \delta(HCC)_{ring}$
1224	1225	1232	$\delta(HCS)_{ring} + \delta(HCC)_{ring}$
1199	1199	1203	$\nu(CC)_{enone} + \delta(CCC)_{ring}$
1169		1185	$\nu(CC)_{ring} + \delta(HCC)_{enone} + \delta(HCC)_{ring}$
1106	1095	1115	$\nu(CC)_{ring} + \nu(CC)_{enone} + \delta(CCC)_{ring}$
1095	1088	1079	$\nu(CC)_{enone} + \delta(HCS)_{ring} + \delta(HCC)_{ring}$
1045	1047	1034	$\nu(CC)_{ring} + \delta(HCC)_{ring}$
1038	1041	1025	$\nu(CC)_{ring} + \delta(CCC)_{ring} + \delta(HCC)_{ring}$
967		977	τ(HCenoneCenoneCring) + τ(HCenoneCringCring)
959	963	950	$\nu(CC)_{enone} + \delta(CCC)_{enone}$
873		881	$\tau(HCSC)_{ring} + \tau(HCCC)_{ring} + \tau(CCCC)_{ring}$
856		867	$\tau(HCCC)_{enone} + \gamma(OCCC)_{enone}$
836		837	$\nu(SC)_{ring} + \delta(CCC)_{ring}$
814	815	825	$\tau(HCCC)_{enone} + \tau(HCCC)_{ring}$
	788	801	$\delta(OCC)_{enone} + \delta(CCC)_{enone}$
727		727	$\nu(SC)_{ring} + \delta(CCC)_{ring}$
711	705	716	$\nu(SC)_{ring} + \delta(CCC)_{ring}$
681	680	679	$\delta(OCC)_{enone} + \delta(CCC)_{ring} + \delta(SCC)_{ring}$
666		675	$\tau(HCSC)_{ring} + \gamma(OCCC)_{enone}$
579		584	$\nu(SC)_{ring} + \delta(CCC)_{ring} + \delta(SCC)_{ring}$
564		559	$\tau(CCCC)_{ring} + \tau(SCCC)_{ring}$
503	504	480	$\delta(CCC)_{enone}$
477		478	$\tau(CCCC)_{ring} + \tau$(CringCringCringCenone) + $\tau(SCCC)_{ring}$
397		375	$\delta(CCC)_{enone} + \delta$(CringCringCenone) + δ(CenoneCringS)
314		303	τ(CringCringCringCenone) + $\tau(CCCC)_{enone} + \tau(SCCC)_{ring}$
264		263	$\delta(OCC)_{enone} + \delta(CCC)_{enone} + \delta$(CenoneCringS)
191	197	196	$\tau(CCCC)_{enone}$
	71	88	lattice

below. A conformation consistent with C1 model, shown by calculated Raman profile, is corroborated by the fact that the experimental dipole moment measured previously [37] (3.19D) is closer to the theorical calculated C1 value (3.11D) than C0 (4.15D) and C2 (1.98D).

Table 1 comprises the Raman and IR data for DB thiophene, as well as the corresponding assignments. The calculated vibrational wavenumbers and Potential Energy Distribution (PED) analysis, for all three conformers of the compound, are comprised in Tables S1, S2 and S3 (Supplementary information).

The IR absorptions in the 3020-3100 cm^{-1} region arise from the CH stretching vibrations. In this region the Raman spectrum shows two bands, at 3088 and 3074 cm^{-1}, both assigned to CH stretching modes of the thiophene rings. Two other Raman bands at 3012 and 2990 cm^{-1} are due to the antisymmetric and symmetric olefinic CH stretching modes, respectively.

In the fingerprint region, there are two weak Raman bands at 1658 and 1604 cm^{-1}. The former was assigned as a combination of stretching modes of the carbonyl group and of the C=C bonds, while the latter was attributed to stretching of CC bonds. A very strong Raman band at 1567 cm^{-1} was assigned to a combination of the carbonyl and C=C stretchings. For curcumin, the intense band related to the diketone stretching mode is recorded at 1626 cm^{-1} [38]. On the IR spectrum, said bands appear at 1662, 1602 and 1562 cm^{-1}, respectively.

A strong Raman band at 1419 cm^{-1} was assigned to a combination of ν(CC) and δ(HCC) bands of the thiophene rings. Accordingly, this mode appears at 1425 cm^{-1} in thiophene substituted chalcone [39]. In the IR spectrum, the same mode is seen as a medium intensity absorption at 1419 cm^{-1}.

In the Raman spectrum, two very weak modes occur at 1359 and 1309 cm^{-1}, that were assigned as a combination of ν(CC) and δ(HCS) of the thiophene rings, and as ν(CC)+δ(HCC) of the enone spacers, respectively. The three very weak bands at 1271, 1225 and 1199 cm^{-1} are not visible for the C0 conformer, appearing as very weak bands for the other two. The first one was assigned as HCC bending modes of both enone and thiophene rings, while the second is a combination of δ(HCS) and δ(HCC) of the thiophene atoms. The third band was assigned as ν(CC) of the enone spacer and δ(CCC) of the rings. Three medium intensity features appear at 873, 856 and 836 cm^{-1}: the first two are torsional modes from the rings and the enones, while the last was assigned to a S–C stretching and a C–C–C bending modes. Finally, an isolated weak Raman band at

504 cm^{-1} was ascribed to the bending of the enone group. The equivalent IR band is a medium absorption at 503 cm^{-1}.

3.3. Efflux pump modulation

Unlike the standard inhibitors, DB Thiophene did not reveal clinically relevant antibacterial activity, with a MIC ≥4162.60 μM. However, when used in association with norfloxacin against SA-1199 B, significant synergistic effects were noted - DB thiophene was able to reduce the MIC of norfloxacin by 30%. This synergic effect against NorA efflux pump is due to the inhibition of the efflux pump mechanism. That could be confirmed by examining the association of this curcumin derivative with EtBr, since an identical behaviour was observed.

Similar compounds containing the thiophene rings were already tested as inhibitors of the SA-1199 B NorA efflux pump and showed a significant enhancement in the activity of ciprofloxacin, with an increase in the intracellular level of the antibiotic, confirming the mode of action as an EPI [40–42]. In the present experiment, DB thiophene led to an effective reduction of norfloxacin MIC compared to CCCP. When used in conjunction with EtBr, DB thiophene was effective as CPZ, while there was no statistical difference compared to CCCP. To sum up, the essays indicated that DB thiophene seems to be an inhibitor of NorA when co-administered with norfloxacin, and it is more effective than CCCP (Fig. 4a).

The mutant SA-K2068 is recognized as having a multi-drug resistance that is mediated by MepA instead of NorA. The essays show the ability of DB thiophene to inhibit the MepA efflux pump,

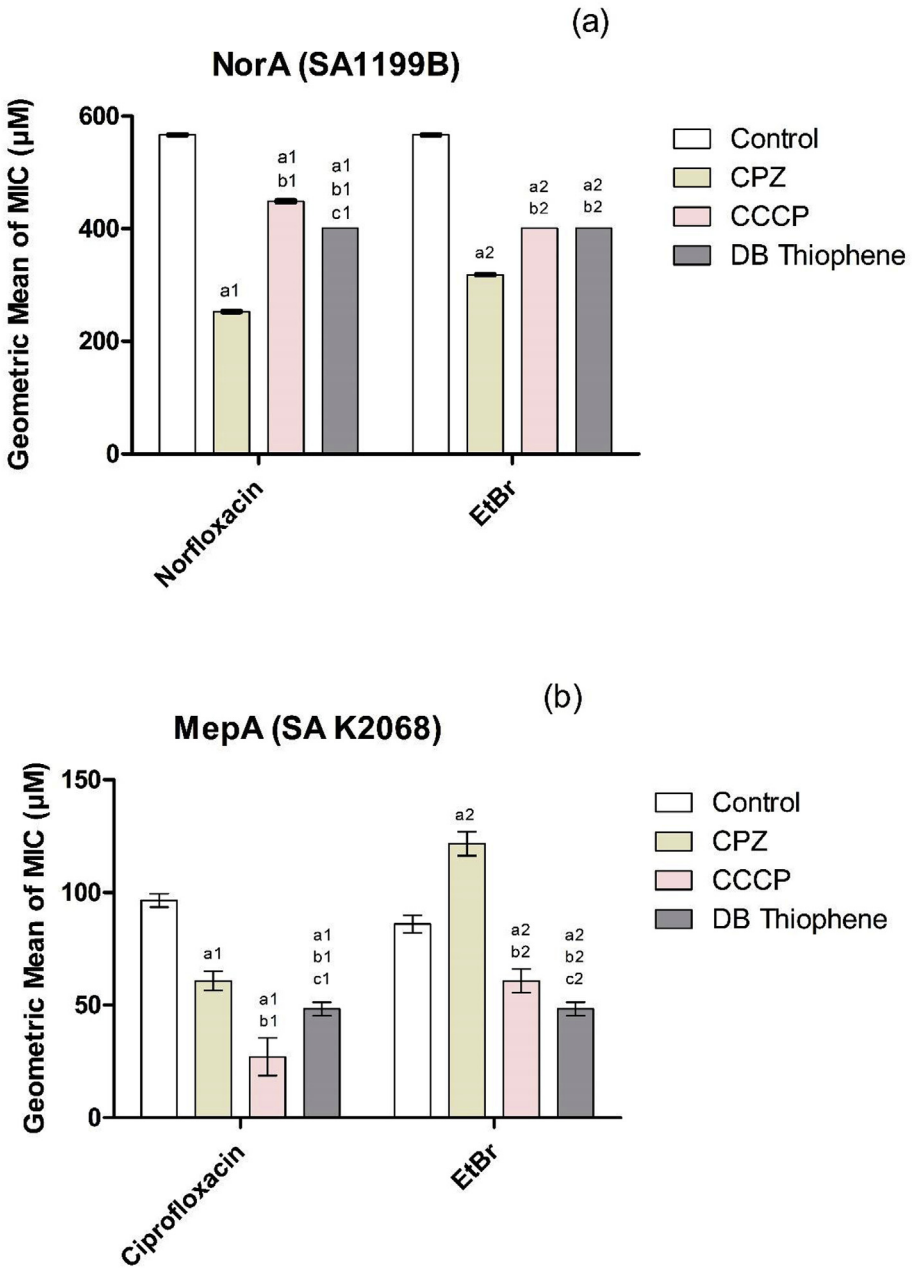

Fig. 4. (a) MIC of Norfloxacin and EtBr, in association with the standard inhibitors and in association with DB thiophene against the strain *S. aureus* 1199 B. $^{a1,a2}p < 0.0001$ *vs* control, $^{b1,b2}p < 0.0001$ *vs* CPZ, $^{c1,c2}p < 0.0001$ *vs* CCCP. (b) MIC of Ciprofloxacin and EtBr, in association with the standard inhibitors and in association with DB thiophene against the strain *S. aureus* K2068. $^{a1,a2}p < 0.0001$ *vs* control, $^{b1,b2}p < 0.0001$ *vs* CPZ, $^{c1,c2}p < 0.0001$ *vs* CCCP (bottom).

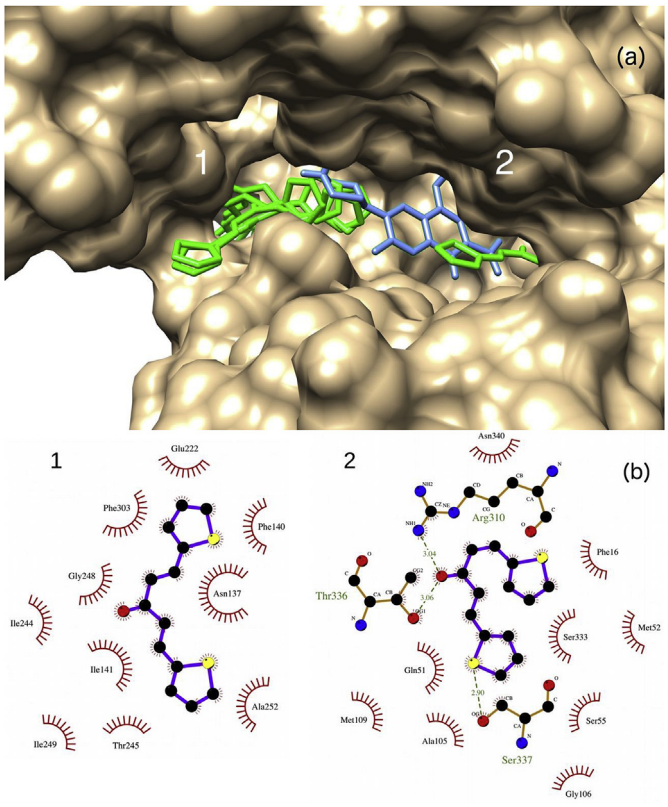

Fig. 5. (a) The best five poses of DB Thiophene (green) and the best pose of norfloxacin (blue) on the binding site of the NorA model. Regions on the binding site are marked 1 and 2. (b) 2D ligand-protein interaction diagram of DB Thiophene and the NorA model on regions 1 and 2.

with a two-fold reduction in MIC of ciprofloxacin. This is a remarkable result since DB thiophene performed better than CPZ, although it was not as effective as CCCP (Fig. 4b). We can't make direct comparisons with other curcumin derivatives, since, to the best of our knowledge, there are no studies on NorA or MepA efflux pump inhibition involving other curcuminoids. The mechanism by which DB thiophene inhibits the NorA or MepA efflux pumps can be explored by molecular docking (to be discussed further on).

3.4. Docking results

Fig. 5a shows the five best poses of DB Thiophene, inserted in the binding site of the NorA model, with energies ranging from −26.527 to −26.276 kJ/mol. For comparison, Li et al. [43] found that the affinity of tetracycline to the same protein was −28.033 kJ/mol. In our simulations, norfloxacin best pose energy was −32.677 kJ/mol. Docking calculations showed that there are two preferred regions in the binding site of the NorA model, labeled regions 1 and 2 (Fig. 5a).

Fig. 5b displays a 2D ligand-protein interaction diagram, with the contact distances in green. The best pose of DB Thiophene is in region 1. In region 2, the C═O group is favorably oriented to form a hydrogen bond with Arg310 (Fig. 5b). Norfloxacin best pose overlaps with poses of DB thiophene in both regions, as can be seen in Fig. 5a. Additionally, and confirming these results, Dantas et al. [44] described the binding site of norfloxacin of a NorA model identical to the one reported here, with interactions with residues 340, 310, 51 and 16. It can thus be argued that DB thiophene hinders the binding of norfloxacin to NorA, being expelled from the bacteria in place of the antibiotic.

All these results suggest that DB Thiophene is likely to function as a competitive inhibitor of NorA efflux protein.

4. Conclusions

The compound (1E,4E)-1,5-Di(thiophen-2-yl)penta-1,4-dien-3-one was synthesised and fully characterised. A study on its vibrational properties was performed using FTIR and FT-Raman spectroscopies as well as quantum chemical calculations at the DFT level (for the three possible conformers of the compound). The experimental and calculated (scaled) vibrational spectra were compared and showed a very good correspondence. These results and the description of the normal modes according to the PED, were used to elucidate the vibrational wavenumber assignments of this synthetic substance. It was shown that this curcuminoid not only inhibits the NorA efflux pump, but also the MepA, thus being a potential new EPI. DB Thiophene interacts with the binding site of efflux pump models and it's likely that DB Thiophene acts as a competitive inhibitor of efflux pumps.

Author's Contribution

Mauro M. Oliveira — Investigation, Writing, original draft, Formal analysis, Helcio S. Santos — Investigation, conducted the spectroscopic analysis by NMR, Henrique D. M. Coutinho — Conceptualization, conceived the experimental design of the microbiological studies., Paulo N. Bandeira — Investigation, performed the synthesis of the compound, Priscila T. da Silva — Investigation, performed the synthesis of the compound, Thiago S. Freitas — Investigation, conducted the efflux pump inhibition assays, Janaina E. Rocha — Investigation, conducted the efflux pump inhibition assays, Jaize C. Xavier — Investigation, carried out the antibacterial assays, Fabia F. Campina — Investigation, carried out the antibacterial assays, Cristina R. S. Barbosa — Investigation, carried out the antibacterial assays, José B. Araújo Neto — Investigation, carried out the antibacterial assays, Raimundo L. S. Pereira — Investigation, performed modulatory antimicrobial activity assays, Maria M. C. Silva — Investigation, performed modulatory antimicrobial activity assays, Débora F. Muniz — Investigation, performed modulatory antimicrobial activity assays, Alexandre M.R. Teixeira — Investigation, carried out the Raman spectroscopy studies, Vanessa M. Frota — Investigation, conducted the analysis by CG-MS, Tigressa H. S. Rodrigues — Investigation, conducted the analysis by CG-MS, Ana M. Amado — writing and Investigation, reviewed the manuscript and conducted the Raman analysis, Maria P. M. Marques — overviewed the writing, reviewed the manuscript and aided on the Conceptualization, Luis A. E. Batista de Carvalho — supervised the experiments, reviewed manuscript, Carlos E. S. Nogueira — Investigation, carried out the DFT calculations, supervised and wrote the original draft

Declaration of competing interests

The authors declare that they have no known competing financial interests or personal relationships that could have appeared to influence the work reported in this paper.

Acknowledgments

Financial support is acknowledged: from the Portuguese Foundation for Science and Technology (FCT) (UIDB/00070/2020).

CENAUREMN - Northeastern Center for the Application and Use of Nuclear Magnetic Resonance and EMBRAPA AGROINDÚSTRIA

TROPICAL-Laboratório Multiusuário de Química de Produtos Naturais.

Appendix A. Supplementary data

Supplementary data to this article can be found online at https://doi.org/10.1016/j.molstruc.2020.128291.

References

[1] A.N. Nurfina, M.S. Reksohadiprodjo, H. Timmerman, U.A. Jenie, D. Sugiyanto, H. Van Der Goot, Synthesis of some symmetrical curcumin derivatives and their antiinflammatory activity, Eur. J. Med. Chem. 32 (1997) 321–328, https://doi.org/10.1016/S0223-5234(97)89084-8.

[2] A. Goel, A.B. Kunnumakkara, B.B. Aggarwal, Curcumin as "Curecumin": from kitchen to clinic, Biochem. Pharmacol. 75 (2008) 787–809, https://doi.org/10.1016/j.bcp.2007.08.016.

[3] I. Chattopadhyay, K. Biswas, U. Bandyopadhyay, R.K. Banerjee, Turmeric and curcumin: biological actions and medicinal applications, Curr. Sci. 87 (2004) 44–53.

[4] A. Mazumder, K. Raghavan, J. Weinstein, K.W. Kohn, Y. Pommier, Inhibition of human immunodeficiency virus type-1 integrase by curcumin, Biochem. Pharmacol. 49 (1995) 1165–1170, https://doi.org/10.1016/0006-2952(95)98514-A.

[5] M.A. Tomren, M. Másson, T. Loftsson, H.H. Tønnesen, Studies on curcumin and curcuminoids. XXXI. Symmetric and asymmetric curcuminoids: stability, activity and complexation with cyclodextrin, Int. J. Pharm. 338 (2007) 27–34, https://doi.org/10.1016/j.ijpharm.2007.01.013.

[6] G. Liang, L. Shao, Y. Wang, C. Zhao, Y. Chu, J. Xiao, Y. Zhao, X. Li, S. Yang, Exploration and synthesis of curcumin analogues with improved structural stability both in vitro and in vivo as cytotoxic agents, Bioorg. Med. Chem. 17 (2009) 2623–2631, https://doi.org/10.1016/j.bmc.2008.10.044.

[7] V. Basile, E. Ferrari, S. Lazzari, S. Belluti, F. Pignedoli, C. Imbriano, Curcumin derivatives: molecular basis of their anti-cancer activity, Biochem. Pharmacol. 78 (2009) 1305–1315, https://doi.org/10.1016/j.bcp.2009.06.105.

[8] G. Liang, S. Yang, L. Jiang, Y. Zhao, L. Shao, J. Xiao, F. Ye, Y. Li, X. Li, Synthesis and anti-bacterial properties of mono-carbonyl analogues of curcumin, Chem. Pharm. Bull. (Tokyo) 56 (2008) 162–167, https://doi.org/10.1248/cpb.56.162.

[9] C. Zhao, Y. Zhang, P. Zou, J. Wang, W. He, D. Shi, H. Li, G. Liang, S. Yang, Synthesis and biological evaluation of a novel class of curcumin analogs as anti-inflammatory agents for prevention and treatment of sepsis in mouse model, Drug Des. Dev. Ther. 9 (2015) 1663–1678, https://doi.org/10.2147/DDDT.S75862.

[10] B.W. Ho, W.S. Shin, S. Lee, M.A. Chan, Synthesis of novel curcumin mimics with asymmetrical units and their anti-angiogenic activity, Bioorg. Med. Chem. Lett 15 (2005) 3782–3786, https://doi.org/10.1016/j.bmcl.2005.05.064.

[11] S.S. Costa, M. Viveiros, L. Amaral, I. Couto, Multidrug efflux pumps in Staphylococcus aureus: an update, Open Microbiol. J. 7 (2013) 59–71, https://doi.org/10.2174/1874285801307010059.

[12] S.R. Tintino, C.D.M. Oliveira-Tintino, F.F. Campina, R.L.P. Silva, M. do S. Costa, I.R.A. Menezes, J.T. Calixto-Júnior, J.P. Siqueira-Junior, H.D.M. Coutinho, T.C. Leal-Balbino, V.Q. Balbino, Evaluation of the tannic acid inhibitory effect against the NorA efflux pump of Staphylococcus aureus, Microb. Pathog. 97 (2016) 9–13, https://doi.org/10.1016/j.micpath.2016.04.003.

[13] A.A. Neyfakh, C.M. Borsch, G.W. Kaatz, Fluoroquinolone resistance protein NorA of Staphylococcus aureus is a multidrug efflux transporter, Antimicrob. Agents Chemother. 37 (1993) 128–129, https://doi.org/10.1128/AAC.37.1.128.

[14] G.W. Kaatz, S.M. Seo, C.A. Ruble, Mechanisms of fluoroquinolone resistance in staphylococcus aureus, J. Infect. Dis. 163 (1991) 1080–1086, https://doi.org/10.1093/infdis/163.5.1080.

[15] G.W. Kaatz, F. McAleese, S.M. Seo, Multidrug resistance in Staphylococcus aureus due to overexpression of a novel multidrug and toxin extrusion (MATE) transport protein, Antimicrob. Agents Chemother. 49 (2005) 1857–1864, https://doi.org/10.1128/AAC.49.5.1857-1864.2005.

[16] B.D. Schindler, P. Jacinto, G.W. Kaatz, Inhibition of drug efflux pumps in Staphylococcus aureus: current status of potentiating existing antibiotics, Future Microbiol. 8 (2013) 491–507, https://doi.org/10.11250/chemotherapy1953.16.843.

[17] P. Singh, A. Anand, V. Kumar, Recent developments in biological activities of chalcones: a mini review, Eur. J. Med. Chem. 85 (2014) 758–777, https://doi.org/10.1016/j.ejmech.2014.08.033.

[18] L. Claisen, A. Claparède, Condensationen von Ketonen mit Aldehyden, Berichte der Dtsch. Chem. Gesellschaft. 14 (1881) 2460–2468.

[19] J.G. Schmidt, Ueber die Einwirkung von Aceton auf Furfurol und auf Bittermandelöl bei Gegenwart von Alkalilauge, Berichte der Dtsch. Chem. Gesellschaft. 14 (1881) 1459–1461, https://doi.org/10.1002/cber.188101401306.

[20] W. Kohn, L.J. Sham, Self-consistent equations including exchange and correlation effects, Phys. Rev. 140 (1965) A1133–A1138, https://doi.org/10.1103/PhysRev.140.A1133.

[21] D.J.F. M. J. Frisch, G. W. Trucks, H. B. Schlegel, G. E. Scuseria, M. A. Robb, J. R. Cheeseman, G. Scalmani, V. Barone, G. A. Petersson, H. Nakatsuji, X. Li, M. Caricato, A. Marenich, J. Bloino, B. G. Janesko, R. Gomperts, B. Mennucci, H. P. Hratchian, J. V. Ort, Gaussian 09, Revision A.02, ([s.d.]).

[22] P.J. Stephens, F.J. Devlin, C.F. Chabalowski, M.J. Frisch, Ab initio calculation of vibrational absorption and circular dichroism spectra using density functional force fields, J. Phys. Chem. 98 (1994) 11623–11627, https://doi.org/10.1021/j100096a001.

[23] NIST Computational Chemistry Comparison and Benchmark Database, ([s.d.]) doi:10.18434/T47C7Z.

[24] M.H. Jamróz, Vibrational energy distribution analysis (VEDA): scopes and limitations, spectrochim, Acta Part A Mol. Biomol. Spectrosc. 114 (2013) 220–230, https://doi.org/10.1016/J.SAA.2013.05.096.

[25] M.A. Wikler, Methods for dilution antimicrobial susceptibility tests for bacteria that grow aerobically: approved standard, CLSI 26 (2006). M7–A7.

[26] H. Yoshida, M. Bogaki, S. Nakamura, K. Ubukata, M. Konno, Nucleotide sequence and characterization of the Staphylococcus aureus norA gene, which confers resistance to quinolones, J. Bacteriol. 172 (1990) 6942–6949, https://doi.org/10.1128/jb.172.12.6942-6949.1990.

[27] G.W. Kaatz, S.M. Seo, C.A. Ruble, Efflux-mediated fluoroquinolone resistance in Staphylococcus aureus, Antimicrob. Agents Chemother. 37 (1993) 1086–1094, https://doi.org/10.1128/AAC.37.5.1086.

[28] P. Petersen, A. Ruzin, S.J. Projan, E. Murphy, P.A. Bradford, F. McAleese, P.M. Dunman, A novel MATE family efflux pump contributes to the reduced susceptibility of laboratory-derived Staphylococcus aureus mutants to tigecycline, Antimicrob. Agents Chemother. 49 (2005) 1865–1871, https://doi.org/10.1128/aac.49.5.1865-1871.2005.

[29] J.M. Pagès, M. Masi, J. Barbe, Inhibitors of efflux pumps in Gram-negative bacteria, Trends Mol. Med. 11 (2005) 382–389, https://doi.org/10.1016/j.molmed.2005.06.006.

[30] M. Malléa, J. Chevalier, A. Eyraud, J.M. Pagès, Inhibitors of antibiotic efflux pump in resistant Enterobacter aerogenes strains, Biochem. Biophys. Res. Commun. 293 (2002) 1370–1373, https://doi.org/10.1016/S0006-291X(02)00404-7.

[31] S. Sabatini, G.W. Kaatz, G.M. Rossolini, D. Brandini, A. Fravolini, From phenothiazine to 3-phenyl-1,4-benzothiazine derivatives as inhibitors of the Staphylococcus aureus NorA multidrug efflux pump, J. Med. Chem. 51 (2008) 4321–4330, https://doi.org/10.1021/jm701623q.

[32] G.W. Kaatz, V.V. Moudgal, S.M. Seo, J.E. Kristiansen, Phenothiazines and thioxanthenes inhibit multidrug efflux pump activity in Staphylococcus aureus, Antimicrob. Agents Chemother. 47 (2003) 719–726, https://doi.org/10.1128/AAC.47.2.719-726.2003.

[33] GraphPad Software, La Jolla California USA, ([s.d.]).

[34] A. Waterhouse, M. Bertoni, S. Bienert, G. Studer, G. Tauriello, R. Gumienny, F.T. Heer, T.A.P. de Beer, C. Rempfer, L. Bordoli, R. Lepore, T. Schwede, SWISS-MODEL: homology modelling of protein structures and complexes, Nucleic Acids Res. 46 (2018) W296–W303., https://doi.org/10.1093/nar/gky427.

[35] G.M. Morris, R. Huey, W. Lindstrom, M.F. Sanner, R.K. Belew, D.S. Goodsell, A.J. Olson, AutoDock4 and AutoDockTools4: automated docking with with selective receptor flexibility, J. Comput. Chem. 30 (2010) 2785–2791, https://doi.org/10.1002/jcc.21256.

[36] S. Murugavel, G. Ganesh, A. SubbiahPandi, R. Murugan, S. SrimanNarayanan, (E,E)-1,5-Di-2-thienylpenta-1,4-dien-3-one, International Union of Crystallography, 2008, https://doi.org/10.1107/S1600536808026603.

[37] S.V. Tseukerman, V.M. Nikitchenko, V.D. Orlov, V.F. Lavrushin, Dipole moments OF thiophene OF chalcones and their VINYLOGS, Chem. Heterocycl. Compd. 3 (1967) 232–238.

[38] P.R.K. Mohan, G. Sreelakshmi, C.V. Muraleedharan, R. Joseph, Water soluble complexes of curcumin with cyclodextrins: characterization by FT-Raman spectroscopy, Vib. Spectrosc. 62 (2012) 77–84, https://doi.org/10.1016/j.vibspec.2012.05.002.

[39] T.A. de Toledo, R.C. da Costa, H.M. Al-Maqtari, J. Jamalis, P.S. Pizani, Temperature dependence of the Raman spectrum of 1-(4-chlorophenyl)-3-(2-thienyl) prop-2-en-1-one, Spectrochim. Acta Part A Mol. Biomol. Spectrosc. 180 (2017) 9–17, https://doi.org/10.1016/j.saa.2017.02.051.

[40] J. Fournier dit Chabert, B. Marquez, L. Neville, L. Joucla, S. Broussous, P. Bouhours, E. David, S. Pellet-Rostaing, B. Marquet, N. Moreau, M. Lemaire, Synthesis and evaluation of new arylbenzo[b]thiophene and diarylthiophene derivatives as inhibitors of the NorA multidrug transporter of Staphylococcus aureus, Bioorg. Med. Chem. 15 (2007) 4482–4497, https://doi.org/10.1016/j.bmc.2007.04.023.

[41] F. Liger, P. Bouhours, C. Ganem-Elbaz, C. Jolivalt, S. Pellet-Rostaing, F. Popowycz, J.M. Paris, M. Lemaire, C2 arylated benzo[b]thiophene derivatives as Staphylococcus aureus NorA efflux pump inhibitors, ChemMedChem 11 (2016) 320–330, https://doi.org/10.1002/cmdc.201500463.

[42] S. Alibert, J. Pagès, Efflux pump inhibitors in bacteria, Expert Opin. Ther. Pat. 17 (2007) 883–888, https://doi.org/10.1517/13543776.17.8.883.

[43] Y. Li, Z.T. Cao, X.Y. Wang, X.Z. Ge, Expression of the TetA gene encoding TetA efflux protein in E. coli contributes to its increased bacterial resistance toward berberine, J. Asian Nat. Prod. Res. 20 (2018) 374–384, https://doi.org/10.1080/10286020.2017.1384818.

[44] N. Dantas, T.M. de Aquino, J.X. de Araújo-Júnior, E. da Silva-Júnior, E.A. Gomes, A.A.S. Gomes, J.P. Siqueira-Júnior, F.J.B. Mendonça Junior, Aminoguanidine hydrazones (AGH's) as modulators of norfloxacin resistance in Staphylococcus aureus that overexpress NorA efflux pump, Chem. Biol. Interact. 280 (2018) 8–14, https://doi.org/10.1016/j.cbi.2017.12.009.